



ARTIFICIAL NEURAL NETWORKS FOR CONTROL OF THREE PHASE GRID CONNECTED PV SYSTEM

Avinash shukla, M.Tech Student, Department of Electrical and Electronics Engineering, Al Falah University, Faridabad, Haryana, India.

Mati ur rehman, Associate Professor, Department of Electrical and Electronics Engineering, Al Falah University, Faridabad, Haryana, India.

ABSTRACT

Traditionally, normal decoupled d-q vector control techniques have been used to regulate grid-connected converters. Recent research, however, suggests that these kinds of techniques have limits when it comes to how well they work with dynamic systems. This research explores the use of a neural network to regulate a grid-connected rectifier/inverter in order to mitigate such limits. The neural network uses back-propagation across time to train itself and implements a dynamic programming technique. Additional techniques are used to improve performance and stability in the face of disturbances. These techniques include applying grid disturbance voltage to the outputs of a well-trained network and using integrals of error signals to the network inputs.

Keywords: photovoltaic (PV), artificial neural network, maximum power point tracking (MPPT).

Introduction

The need for energy around the world is growing at an exponential rate as we go into the twenty-first century. It is anticipated that this trend would continue far into the future due to economic expansion and increased per capita power usage [1]. There is a significant disadvantage with renewable energy sources, despite the fact that they have the capacity to supply nearly two billion people living in distant places with electricity and meet the world's energy needs [2,3]. The amount of energy they produce fluctuates greatly depending on weather factors, such as photovoltaic systems' solar irradiation. In order to improve these systems' energy efficiency, maximum power point tracking methods must be used. Although traditional methods such as Incremental Conductance, Perturb & Observe, and Hill Climbing Search have been thoroughly investigated in this domain, Artificial Neural Networks (ANNs) have notable benefits concerning precision and the capacity to represent intricate interactions [4,5,6]. Our goal is to develop a novel and dependable control strategy for grid-connected photovoltaic energy conversion systems using artificial neural networks (ANNs). Our main objective is to maximize power extraction and provide effective energy distribution in order to maximize the performance of the PV system. In order to achieve this, we use the voltage-based Perturb and Observe technique, which enables us to continuously modify the PV system's critical point in order to maximize power output. In addition, we include an integral-proportional (PI) controller to efficiently control both active and reactive powers as well as the DC bus voltage[7]. This guarantees the PV system will operate steadily and dependably in a variety of situations. We utilize the capability of Artificial Neural Networks (ANNs) [8,9] to further optimize the production of renewable energy and improve the system's responsiveness to climatic fluctuations. ANNs have several useful features, such as the capacity to effectively and precisely predict complicated relationships and take climate fluctuations into consideration. The system's performance and efficiency can be increased by using ANNs, which will enable it to maximize energy generation from renewable sources and adapt to various environmental circumstances. Variations in internal parameters or possible modeling mistakes are taken into consideration in our study as internal disturbances that must be taken into account and managed within the control system [10,11]. The sustainability and dependability of the PV system are further ensured by closely monitoring and addressing external disturbances like grid instability. We can maximize the PV system's power production, improve energy management, and add to the overall sustainability and efficiency of renewable energy generation by integrating the PI controller, the

voltage-based Perturb and Observe technique, and the use of ANNs. The paper is divided into four primary sections. The introduction gives a quick overview of the subject at hand. The photovoltaic system's modeling is the main topic of the second section. The controllers and mathematical models used in our investigation are described in the third section[12]. The fourth and last section provides a thorough analysis of the results and shows the simulation outcomes.

System Modeling:

One of the many parts of the system shown in Fig. 1 is a photovoltaic (PV) system that is made to work in a variety of weather conditions. Power exchange is possible between two-stage power electronics converters, namely an inverter and a boost converter, connected by a DC bus. In order to reduce the overall harmonic distortion in the current, the inverter is connected to the electrical grid via a 35 kV step-up transformer and a three-phase RL filter [13].

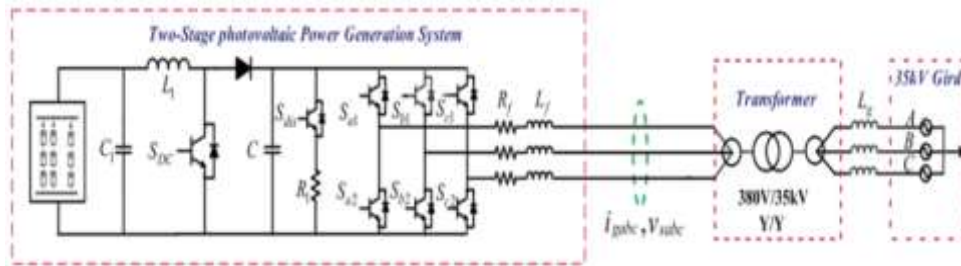


Fig. 1. Grid-Connected Photovoltaic System

Fig.2 depicts the electrical equivalent to a photovoltaic cell, which consists of a current source that is produced by light, two diodes (D1, D2), and series (R_s) and parallel resistors (R_{sh}). The following equation explains how a solar cell's current-voltage relationship works [14]:

$$I_{pv} = I_{ph} - I_{d1} - I_{d2} - I_{sh} \tag{1}$$

$$I_{d1} = I_{01} \left[e^{\frac{V_{pv} + R_s I_{pv}}{\beta_1 V_T}} - 1 \right] \tag{2}$$

$$I_{d2} = I_{02} \left[e^{\frac{V_{pv} + R_s I_{pv}}{\beta_2 V_T}} - 1 \right] \tag{3}$$

$$I_{sh} = \frac{V_{pv} + R_s I_{pv}}{R_s} \tag{4}$$

$$V_T = \frac{KT}{q} \tag{5}$$

Where T is temperature of the cell (K), q is the electronic charge (C), I_{pv} is the current output (A) of the solar cell, is its voltage at output (V), I_{ph} is the current generated by light (A), I_{01} and I_{02} are the first and second diodes' respective reverse saturation currents (in amps), V_T is the cell thermal voltage, and β_1 and β_1 are the first and second diodes' respective dimensionless ideal.

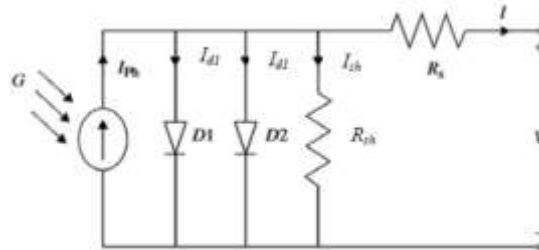


Fig. 2. Equivalent cell electrical circuit

Grid Side Converter Model (GSC):

The equations on the grid side can be expressed as [16]:

$$V_{g,ab,c} = V_{ia,b,c} + R_f i_{ga,b,c} + L_f \frac{di_{ga,b,c}}{dt} \tag{6}$$

After applying the d-q transformation, equation (7) is transformed into the following form:

$$V_{id} = V_{gd} + R_f i_{gd} + L_f \frac{di_{gd}}{dt} - L_f \omega_g i_{iq} \quad (7)$$

$$V_{iq} = V_{gd} + R_f i_{gq} + L_f \frac{di_{gq}}{dt} - L_f \omega_g i_{iq} \quad (8)$$

In this context, the direct and quadrature elements of the grid voltage are denoted as V_{gd} and V_{gq} , while the direct and quadrature elements of the grid current are represented by i_{gd} and i_{gq} . Additionally, V_{id} and V_{iq} correspond to the direct and quadrature components of the source inverter voltage, respectively. R_f and L_f refer to the resistance and inductance of the filter, respectively, and $\omega_g = 2 \cdot \pi \cdot fg$, fg , which is determined through the Phase Locked Loop (PLL)[19].

The equations showed previously able to be expressed in the following form:

$$\frac{di_{gd}}{dt} = -\lambda_1 \cdot i_{gd} - \omega_g i_{gq} + \lambda_2 (v_{id} - v_{gd}) \quad (9)$$

$$\frac{di_{gq}}{dt} = -\lambda_1 \cdot i_{gq} - \omega_g i_{gd} + \lambda_2 (v_{iq} - v_{gq}) \quad (10)$$

By defining λ_1 as R_f/L_f and λ_2 as $1/L_f$, the expressions can be rewritten as follows. The active and reactive powers (P_g , Q_g) injected inside the grid are calculated using the following equations:

$$P_g = 3/2(v_{gd} \cdot i_{gd} - v_{gq} \cdot i_{gq}) \quad (11)$$

$$Q_g = 3/2(v_{gq} \cdot i_{gd} - v_{gd} \cdot i_{gq}) \quad (12)$$

The following is an expression for the DC-Link voltage equation:

$$C_b \frac{dV_{dc}}{dt} = i_{dc} = i_s - i_g \quad (13)$$

Where V_{dc} stands for the DC-Link's voltage, i_{dc} for the current flowing through it, and C for the capacitance of the DC-Link capacitor. Moreover, i_s and i_g refer to the current flowing through the PV-boost side and the grid side, respectively.

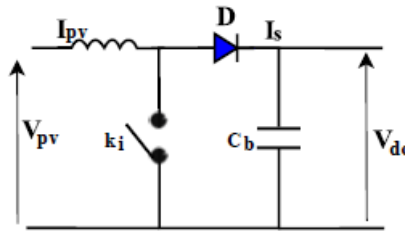


Fig. 3. Boost converter

Fig. 3 illustrates a boost converter placed in between the inverter and the PV panel. Its objective is to raise a solar panel's voltage in accordance with the duty cycle (α)[10]. The relationship between the duty cycle, the converter's outputs, and the outputs of the PV panel—which serves as the converter's input—is explained as follows:

$$\text{Output voltage of Boost converter} = \frac{1}{1-\alpha} V_{pv} \quad (14)$$

$$\text{Output current of Boost converter} = I_{pv} (1 - \alpha) \quad (15)$$

Inductor and capacitor can be calculated as;

$$L_{pv} = \frac{\alpha}{\Delta I_{pv} f_s} V_{pv} \quad (16)$$

$$\text{Capacitor value} = \frac{\alpha}{\Delta V_{pv} f_s} i_{grid} \quad (15)$$

Artificial Neural Network:

Powerful tools include artificial neural networks for modeling nonlinear functions and exhibit remarkable universal capabilities. One of the major strengths of ANNs is their capacity for learning and improving their performance through training data. At their core, ANNs consist of neurons which function as computing nodes. Each neuron multiplies the input signals by constant weights, adds the products, applies a nonlinear function, and then transfers the output to an activation function, as

depicted in Fig.4. According to previous research, the mathematical representation of a neuron may be stated [17, 18]:

$$Y = \varphi(\sum_{i=1}^N W_i \cdot X_i + b) \tag{18}$$

In this context, the model of a neuron can be described mathematically as follows: the neuron's input signals are represented by (X_1, X_2, \dots, X_N) , while (W_1, W_2, \dots, W_N) correspond to the weights associated with each input signal. Additionally, Y is the neuron's output signal, b is bias parameter, and φ denotes a tangent sigmoid function.

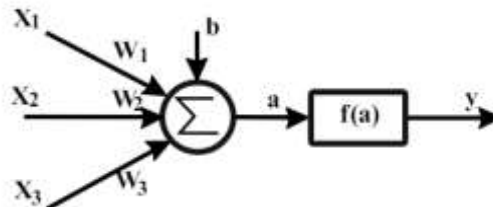


Fig. 4. Artificial neuron representation

Photovoltaic systems are characterized by power-voltage (P-V) and current-voltage (I-V) nonlinear curves, which exhibit a unique maximum power point (MPP). To optimize performance, the P&O algorithm adjusts the reference voltage according to changes in the power-to-voltage ratio. In this approach, the optimum reference voltage for the ANN controller is created using an adaptive and variable-step P&O approach, as illustrated in Fig.5.

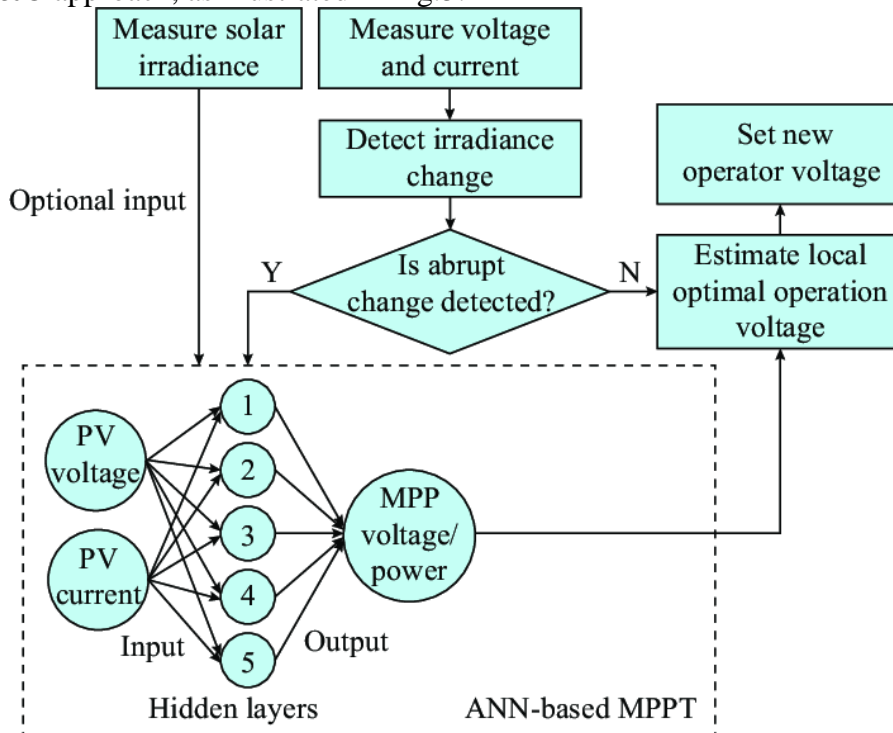


Fig. 5. Structure of an ANN-based MPPT

The optimal reference voltage derived from this MPPT technique is highly effective, as it can maintain minimal voltage variation around the MPP. To enhance the robustness of the system, an ANN-based control loop is proposed to track the MPP even in the face of environmental changes. To create the ANN controller using Matlab/Simulink, we have selected hidden layers for the MPPT controller, as depicted in Fig.6. The activation functions used for the hidden layers and the output layer are "tansig" and "purelin," respectively. The weights and biases of this network are updated using the Levenberg-Marquardt (LM) algorithm, which is a back propagation algorithm. The external loop incorporates an adaptive P&O technique to regulate the V_{pv} voltage and achieve the reference voltage, as illustrated in Fig.7 [15-17].

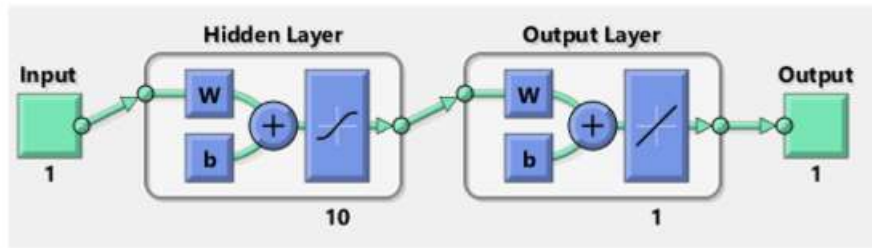


Fig. 6. Neural network diagram

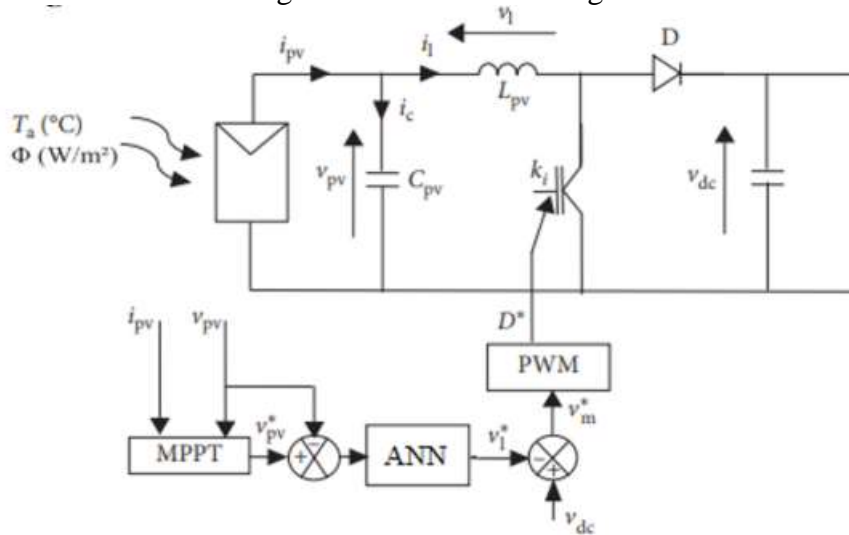


Fig. 7. P&O-based ANN-MPPT

Results:

The results of our simulation tests, which tested our suggested control approach for a 100-kW photovoltaic system linked to a three-phase electrical grid with a voltage of 380V and frequency of 50Hz (the system's specifications are listed in the Appendix), are shown in this section. The system consists of a voltage-controlled inverter with VOC (Voltage Oriented Control) control, a boost converter using ANN-based MPPT control, and a three-phase RL filter that reduces the total harmonic distortion (THD) of the injected current while maintaining a dependable connection to the power grid. The simulation results shown in Fig. 8-14 show how successful the suggested control approach is. In particular, the solar system's power output was successfully increased through the use of the Artificial Neural Network (ANN) approach. This suggests that the system was able to produce the most energy feasible thanks to the ANN technique. Our ANN-based MPPT system has a fast response time, which enables the photovoltaic system to swiftly adjust to changes in solar radiation levels and boosts the efficiency of energy production.

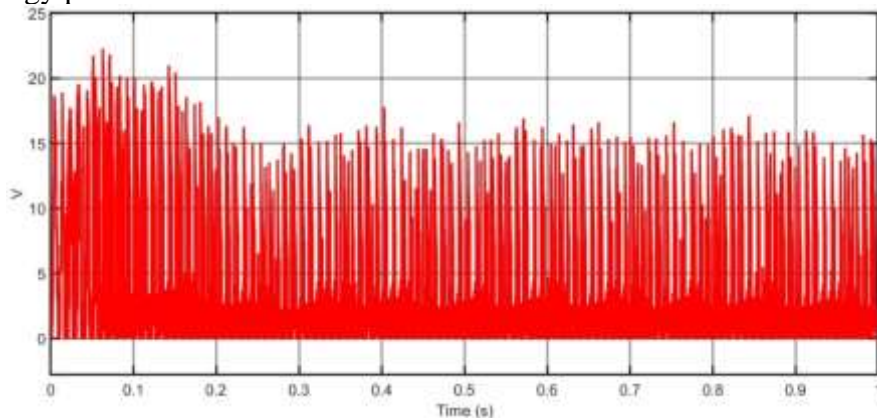


Fig-8 Solar Voltage

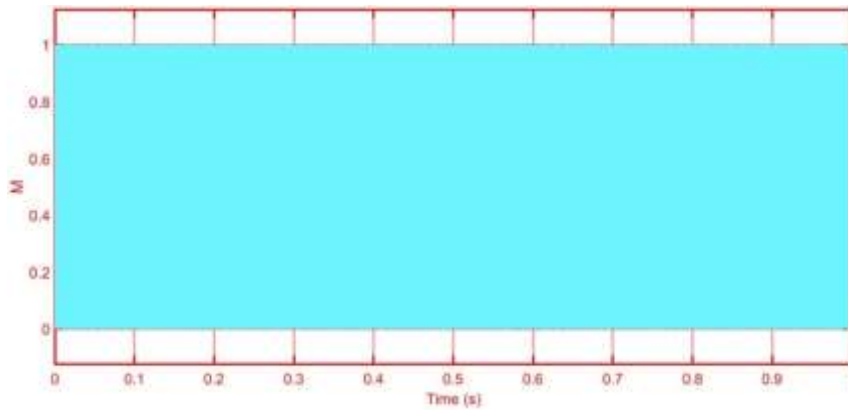


Fig-9 ANN-based MPPT generated Pulse

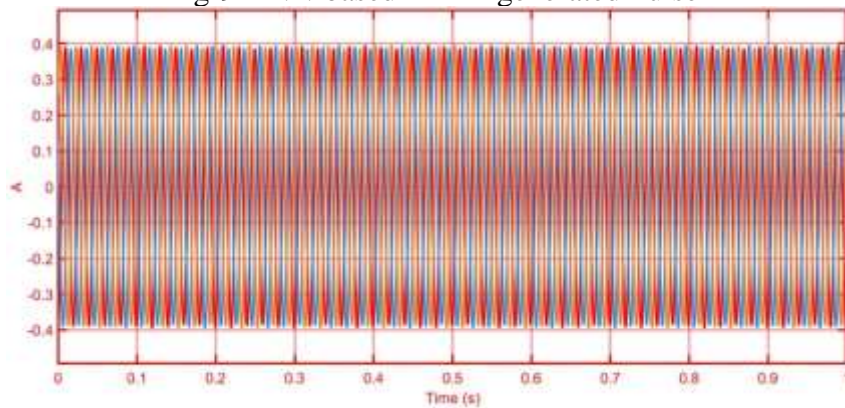


Fig- 10 Grid current

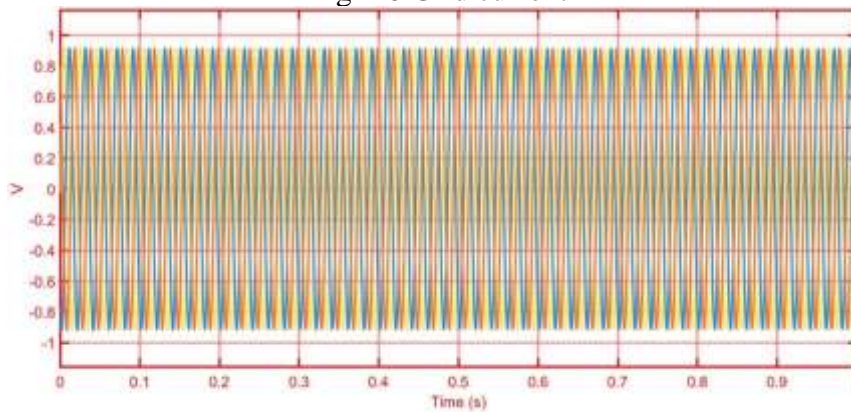


Fig-11 Grid Voltage

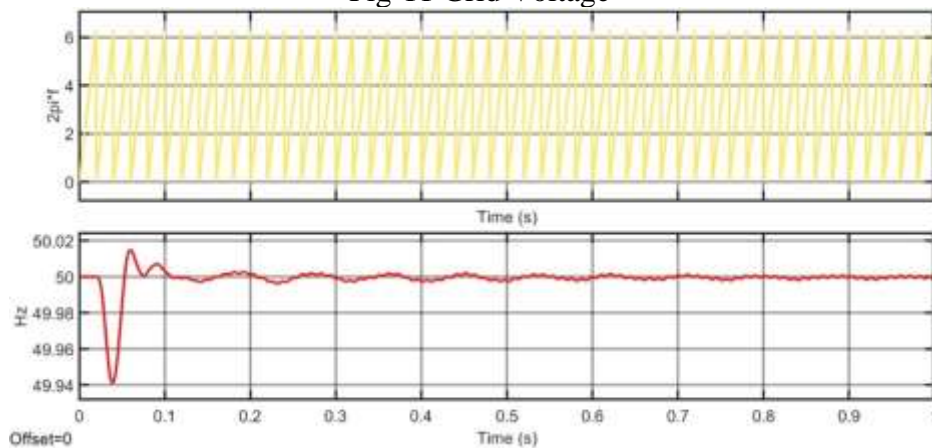


Fig-12 Grid frequency (With ANN-based MPPT)

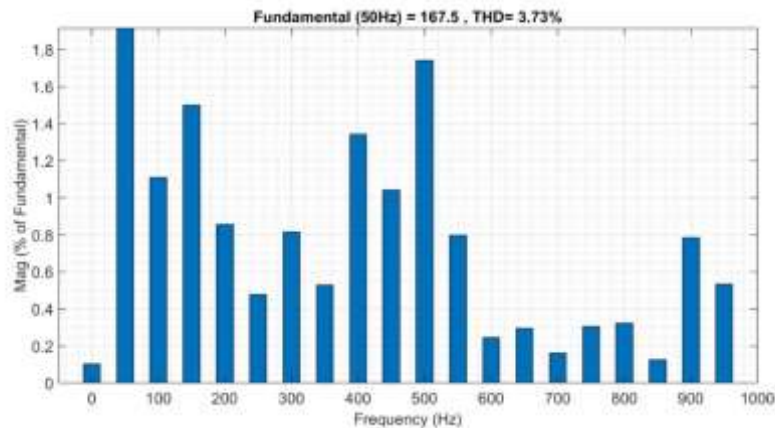


Fig- 13 THD in load voltage

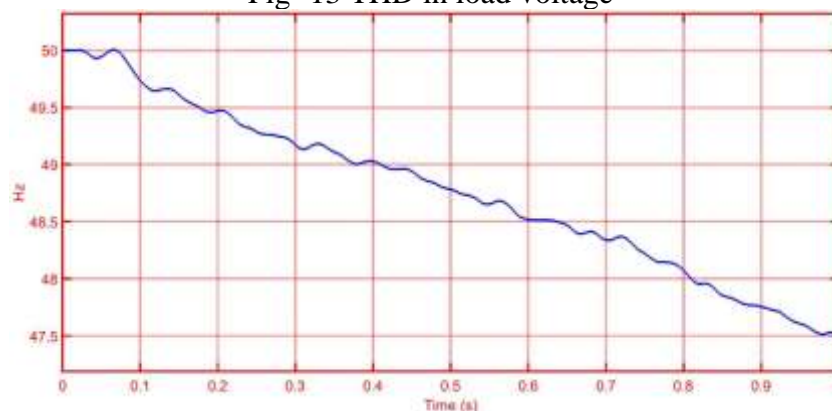


Fig-14 Grid frequency (Without ANN-based MPPT at high load)

Conclusion:

Our study's objective was to create a reliable control plan for a solar system that is connected to the grid by using two different controllers: an Artificial Neural Network (ANN) controller. We were able to optimize the PV system's power production through the use of the ANN-MPPT (Maximum Power Point Tracking) technique, which resulted in increased efficiency and quicker reaction times. Our investigation verified that the PV system's active and reactive powers were successfully managed, guaranteeing that all of the electricity it produced was efficiently fed into the grid. We also set the reactive power to zero, which improved system performance much more and allowed us to reach a power factor almost equal to unity. Overall, our results demonstrate that the suggested control method effectively maximizes the output of grid-connected solar energy systems.

Reference:

[1] Madalina Mihaela Buzau, Javier Tejedor-Aguilera, Pedro Cruz-Romero and Antonio Gómez-Expósito, "Detection of Non-Technical Losses Using Smart Meter Data and supervised Learning", IEEE TRANSACTIONS ON SMART GRID, VOL. 10, NO. 3, MAY 2019

[2] Soham Chatterjee, Vaidheeswaran Archana, Karthik Suresh, Rohit Saha, Raghav Gupta and Fenil Doshi, "Detection of Non-Technical Losses using Advanced Metering Infrastructure and Deep Recurrent Neural Networks", 2017 IEEE International Conference on Environment and Electrical Engineering and 2017 IEEE Industrial and Commercial Power Systems Europe (EEEIC / I&CPS Europe)

[3] P. Antmann, "Reducing technical and non-technical losses in the power sector", Background paper for the WBG Energy Strategy, Tech. Rep., Washington, DC, USA: The World Bank, 2009.



- [4] P. Kadurek, J. Blom, J. Cobben, and W. Kling, "Theft detection and smart metering practices and expectations in the Netherlands", in Proc. 2010 IEEE/PES Innovative Smart grid Technologies Conference Europe (ISGT Europe), 2010, pp. 1-6.
- [5] Tanveer Ahmad, "Non-technical loss analysis and prevention using smart meters", *Renewable and Sustainable Energy Reviews* 72 (2017), 573–589.
- [6] Tanveer Ahmad, "Non-technical loss analysis and prevention using smart meters", *Renewable and Sustainable Energy Reviews* 72 (2017) 573–589.
- [7] Soma Shekara Sreenadh Reddy Depuru, Lingfeng Wang, Vijay Devabhaktuni and Nikhil Gudi, "Smart Meters for Power Grid – Challenges, Issues, Advantages and Status", 2011 IEEE/PES Power Systems Conference and Exposition, DOI:10.1016/J.RSER.2011.02.039
- [8] C. Bennett and D. Highfill, "Networking AMI smart meters", in Proc. IEEE Energy 2030 Conference, Atlanta, GA, Nov. 2008, pp. 1 – 8.
- [9] Yasin Kabalci, "A survey on smart metering and smart grid communication ", *Renewable and Sustainable Energy Reviews* 57(2016),302–318.
- [10] Zhou J,Hu RQ, Qian Yi. ,"Scalable distributed communication architectures to support advanced metering infrastructure",*IEEE Trans Smart Grid Parallel and Distrib Syst* 2012;23:1632–42.
- [11] Kuzlu M, Pipattanasomporn M, Rahman S. ,"Communication network requirements for major smart grid applications in HAN, NAN and WAN", *Comput Netw* 2014;67:74–88.
- [12] Fredrik Ege Abrahamsen, Yun Ai and Michael Cheffena ," Communication Technologies for Smart Grid: A Comprehensive Survey", *Sensors* 2021, 21, 8087.
- [13] Antara Mahanta Barua; Pradyut Kumar Goswami, "Smart metering deployment scenarios in India and implementation using RF mesh network", 2017 IEEE International Conference on Smart Grid and Smart Cities (ICSGSC).
- [14] J. H. Oglund, D. Ilcay, S. Karnouskosy, R. Sauterz, and P.Goncalves da Silva, "Using a 6LoWPAN Smart Meter Mesh Network for Event-Driven Monitoring of Power Quality"
- [15] H. Shahinzadeh, A. Hasanalizadeh, "Implementation of Smart Metering Systems: Challenges and Solutions",*Indonesian Journal of Electrical Engineering*, Vol.12, No.7, pp.5104-5109, July 2014.
- [16] Soham Chatterjee, Vaidheeswaran Archana, Karthik Suresh, Rohit Saha, Raghav Gupta and Fenil Doshi, "Detection of Non-Technical Losses using Advanced Metering Infrastructure and Deep Recurrent Neural Networks", 2017 IEEE International Conference on Environment and Electrical Engineering and 2017 IEEE Industrial and Commercial Power Systems Europe (EEEIC / I&CPS Europe)
- [17] Hasim Sak, Andrew Senior, Françoise Beaufays, "Long Short-Term Memory Recurrent Neural Network Architectures for Large Scale Acoustic Modeling", *INTERSPEECH* (2014), pp. 338-342
- [18] Li S, Fairbank M, Johnson C, Wunsch DC, Alonso E, Proaño JL. Artificial neural networks for control of a grid-connected rectifier/inverter under disturbance, dynamic and power converter switching conditions. *IEEE Trans Neural Netw Learn Syst*. 2014 Apr;25(4):738-50. doi: 10.1109/TNNLS.2013.2280906. PMID: 24807951.
- [19] Adetokun BB, Muriithi CM. Application and control of flexible alternating current transmission system devices for voltage stability enhancement of renewable-integrated power grid: A comprehensive review. *Heliyon*. 2021 Mar 11;7(3):e06461. doi: 10.1016/j.heliyon.2021.e06461. PMID: 33748502; PMCID: PMC7966839.